JOURNAL OF CATALYSIS 79, 451–461 (1983)

Photoassisted Water–Gas Shift Reaction over $Pt/TiO_2(100)$

SHOU-CHIN TSAI, CHIA-CHIEH KAO, AND YIP-WAH CHUNG

Department of Materials Science and Engineering, Northwestern University, Evanston, Illinois 60201

Received September 3, 1982; revised October 19, 1982

Sustained production of hydrogen was observed over platinized $TiO_2(100)$ in the presence of water vapor and carbon monoxide with or without uv illumination. The thermal reaction proceeds with an activation energy of 26.3 ± 0.5 kcal/mole and is dominant at temperatures above 400°K. The photoreaction, which dominates at temperatures below 400°K with an activation energy of 7 ± 2 kcal/mole, was extensively studied in this work. In the photoreaction, the hydrogen production rate was found to be independent of water and CO partial pressure in the range of 0.5 to 18 Torr and 0.1 to 10 Torr, respectively. The reaction rate increases monotonically with increasing uv intensity. Platinum coverage study suggested that the periphery of deposited Pt islands is involved in the photogeneration of H_2. A reaction mechanism assuming CO photoreduction of TiO_2 at $Pt–TiO_2$ periphery sites to be the rate-limiting step is proposed that appears to account for all experimental observations.

1. INTRODUCTION

The report on photoassisted decomposition of liquid water by Fujishima and Honda (*1*) has stimulated much work on photodecomposition of liquid water using various semiconducting photo-anodes (*2–4*). The amount of hydrogen produced in some studies (*5*) was over 1.6×10^5 monolayers (here we define one monolayer to be 10^{15} molecules per square centimeter surface area), which greatly exceeds what might come from the decomposition of surface layers of the electrode. The catalytic nature of photoelectrolysis of water is thus well established.

On the other hand, sustained photocatalytic decomposition of gaseous water on semiconductors has been on a less solid footing. Schrauzer and Guth reported the photoassisted decomposition of gas-phase water on TiO_2 powders (*6*). However, the reaction almost stopped after a few hours, and the amount of hydrogen produced was about a monolayer. Van Damme and Hall (*7*) have suggested that such photoproduction of hydrogen from TiO_2 was actually due to reaction of surface hydroxyl groups. On the other hand, Kawai and Sakata (*8*) reported that uv-irradiated TiO_2 powders mixed with RuO_2 led to relatively high yield of D_2 and O_2 from gaseous water (D_2O). They suggested that the addition of RuO_2 helped O_2 evolution on TiO_2 powders. They found that the amount of D_2 and O_2 evolved ($\sim 10^{20}$ molecules) in 1 week of irradiation exceeded the number of possible surface hydroxyls ($\sim 10^{18}$).

It is important to point out that in Kawai and Sakata's work, the D_2 production rate was ~0.33 monolayer/hr, which is very little in comparison with that of liquid-phase reaction in which a H_2 yield as high as 16,000 monolayers was produced in 1 hr (*5*). It is hence reasonable to expect that different reaction mechanisms are involved in the gas-phase and liquid-phase reactions. Van Damme and Hall (*7*) suggested that surface hydroxyl species act only as intermediates for charge trapping and charge transfer in liquid-phase reaction, whereas they undergo direct decomposition in the gas-phase reaction. In their work of photodecomposition of gaseous water reaction,

0021-9517/83/020451-11$03.00/0

Kawai and Sakata (*8*) proposed a reaction mechanism which involves an oxidation–reduction cycle of the TiO_2 powders.

Recently, Sato and White (*9*) reported that sustained hydrogen production was observed over uv-irradiated platinized TiO_2 powders in the presence of both water vapor and CO. The hydrogen production was not sustained, however, in the absence of CO under otherwise the same experimental conditions. It appears that the introduction of CO into the reactant gas serves to remove oxygen from the system by forming CO_2 and to sustain the photoproduction of hydrogen. This oxygen removal process may be an important step in the photodecomposition of water vapor (*8*).

In this report, further detailed study of the photoassisted water–gas shift reaction over platinized $TiO_2(100)$ surface is presented. Working with single crystals of known surface area, we established the catalytic nature of this reaction. Additional information about this reaction was obtained by measuring the reactivity as a function of Pt coverage, uv intensity, and reactant gas partial pressures. Finally, a reaction mechanism is proposed that appears to be consistent with all experimental observations.

2. EXPERIMENTAL

A schematic diagram of the experimental setup is shown in Fig. 1. A six-way-cross reaction cell is attached to a UHV chamber which has a base pressure of 2×10^{-9} Torr and is equipped with an ion sputtering gun and an evaporator. The specimen was held on a gold foil holder that was mounted on one end of a transfer tube. This allows specimen transfer between the UHV chamber and the reaction cell, where all reactions were performed. The reaction cell was isolated from the UHV chamber during the reaction by closing the gate valve between them.

Two $TiO_2(100)$ specimens were used. They were oriented, cut, and polished using standard metallographic techniques. One specimen with a surface area of 0.63 cm^2 and a thickness of 1 mm was prereduced by heating in vacuum at 773°K for 10 hr. The other specimen (area ~1.13 cm^2, thickness ~1 mm) received no reduction treatment. Most studies were made on the reduced

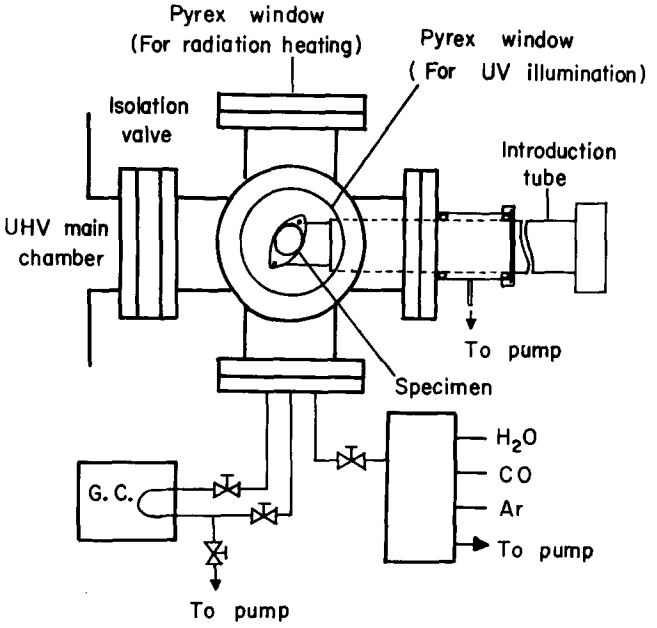

FIG. 1. A schematic diagram of the experimental setup for performing photo and thermal water-gas shift reactions.

TiO_2 specimen. The unreduced specimen was used only for studying the effect of substrate reduction state. The specimens were prepared in the UHV chamber by argon-sputtering with an ion current of 15 μA for 3 min and subsequent annealing at 673°K for 20 min. Although there was no surface analysis device in this chamber to monitor the surface conditions, this treatment was shown to give a clean ordered $TiO_2(100)$-(1 × 3) surface in another chamber. Pt was deposited on the TiO_2 surface using a resistively heated tungsten filament evaporator. The Pt coverage was measured by a quartz crystal thickness monitor which has an ultimate sensitivity of 10^{13} atoms for Pt.

The inner walls of the reaction cell were coated with gold to minimize background reactions. The gas sample was analyzed by a thermal-conductivity gas chromatograph (GC). The sensitivity was enhanced by using a large-volume gas-sampling loop and amplifying the GC output signal. The overall sensitivity after this arrangement is 1 × 10^{14} H_2 molecules produced in the reaction cell. In all reactions, the initial total pressure in the cell was kept constant by pressurizing with argon to 50 Torr to ensure proper gas sampling.

Specimen heating was accomplished by focusing the radiation from a tungsten–halogen lamp onto the specimen surface with its output filtered to cut off the uv. Through a separate window, band-gap radiation was supplied by a high-pressure mercury lamp. The output was filtered with an 8-cm $NiSO_4$ solution (200 g/liter) to remove the infrared and was focused into a beam size of 1.5 cm diameter around the specimen. The photon flux received by the reduced specimen with energies between 3.0 and 3.9 eV (transmission cutoff of Pyrex glass) was measured using a home-made power meter to be ~2 × 10^{16} photons/sec at an input power of 250 W to the lamp.

3. RESULTS

When a platinized $TiO_2(100)$ surface was illuminated with band-gap radiation in the presence of CO and water vapor, hydrogen was produced. Figure 2 shows a typical hydrogen evolution curve as a function of uv illumination time. The reaction was performed over a platinized, reduced TiO_2 (100) (area ~0.63 cm) with a total plati-

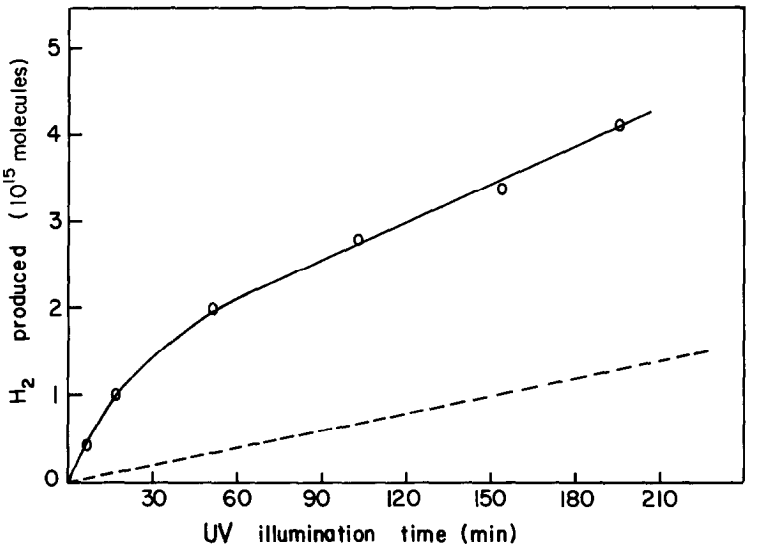

FIG. 2. Hydrogen photoproduction from a platinized $TiO_2(100)$ (1 × 10^{15} Pt atoms) crystal under uv illumination at 363°K in the presence of 18 Torr of water vapor and 0.3 Torr of CO. Background contribution (dashed line) is also included.

num coverage of 1×10^{15} atoms at 363°K in the presence of 18 Torr of water vapor and 0.3 Torr of CO with a uv input power of 250 W. In the following, all reactions were performed under this standard condition unless otherwise stated. From this figure, hydrogen production proceeds with a fast initial rate of $\sim 3.6 \times 10^{15}$ H_2 molecules/hr. The reaction rate decreases with time and attains a rather constant value of 0.9×10^{15} H_2 molecules/hr after 40–50 min. This steady-state reaction rate persisted for at least 3 hr before the experiment was terminated. The transient rate of hydrogen production was found to be independent of the presence or absence of CO. Evacuating the reaction cell in the middle of the experiment followed by letting in new gas mixture did not restore this initial reaction rate while the same steady-state reaction rate was maintained. Due to the possible association of this transient reaction to noncatalytic stoichiometric reaction (*10*), we concentrated on the steady-state reaction in current studies.

Superimposed on Fig. 2 is the hydrogen production from the background. The background reaction was performed by removing the specimen from the holder and carrying out the experiment under otherwise identical experimental conditions. The background reaction showed no initial transient rate and had a constant rate of 0.4×10^{15} H_2 molecules/hr. Although this was a rather large background, repeated runs on both background and Pt/TiO_2 gave very reproducible results. The hydrogen production rate over Pt/TiO_2 was always larger than that of the background. In the remaining sections of this paper, the hydrogen production rate will be given after the background contribution is subtracted.

3.1. Pt coverage dependence. The dependence of the steady-state hydrogen production rate on platinum coverage is shown in Fig. 3. The reaction was performed by

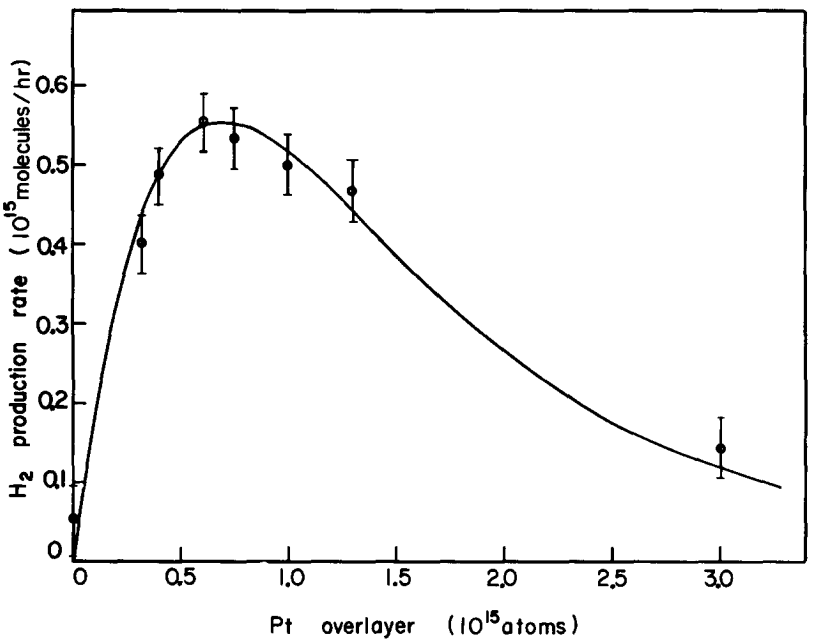

FIG. 3. Hydrogen photoproduction rate as a function of Pt coverage. Hydrogen was produced with band-gap illumination on $Pt/TiO_2(100)$ at 363°K in 18 Torr of water vapor and 0.3 Torr of CO. The continuous curve is a plot of the Pt island perimeter versus Pt coverage obtained by computer simulation, assuming that one Pt monolayer is equivalent to 1.5×10^{15} atoms/cm^2.

varying Pt coverage while keeping other conditions unchanged. The reaction rate increases sharply with increasing Pt coverage and attains a maximum of ~0.55 × 10^{15} H_2 molecules/hr at a total Pt coverage of ~6 × 10^{14} atoms and slowly declines thereafter. This variation of hydrogen production rate as a function of Pt coverage further distinguishes the real photoreaction from the background (which is independent of Pt coverage).

3.2. Temperature dependence. Figure 4 shows the Arrhenius plot of the steady-state hydrogen production rate as a function of temperature with and without band-gap illumination. It is clear from this figure that hydrogen is produced via two distinct reaction pathways, viz., thermal reaction and photoreaction. The thermal reaction proceeds with an activation energy of 26.3 ± 0.5 kcal/mole. It dominates at temperatures above 400°K and is negligible cf. the photoreaction at 363°K. On the other hand, the photoassisted reaction proceeds with a small activation energy of 7 ± 2 kcal/mole. This value is comparable to 7.5 kcal/mole reported by Sato and White (*9*).

3.3. Water vapor pressure and CO pressure dependence. Figure 5 shows the dependence of the steady-state hydrogen photoproduction rate on the water vapor pressure at 363°K, keeping other parameters constant. At P_{CO} = 0.3 Torr, the reaction rate maintains a constant value of 0.5 × 10^{15} H_2 molecules/hr with water vapor pressure between 0.5 and 18 Torr and drops to zero without water vapor. Similar results were obtained for CO pressure dependence experiments as shown in the same figure. At P_{H_2O} = 18 Torr and zero CO partial pressure, the reaction rate is less than 0.1 × 10^{15} H_2 molecules/hr. With CO partial pressure ranging from 0.1 to 10 Torr and P_{H_2O} = 18 Torr the hydrogen production rate keeps a constant value of 0.5 × 10^{15} H_2 molecules/hr.

3.4. Ultraviolet intensity dependence. The dependence of hydrogen production

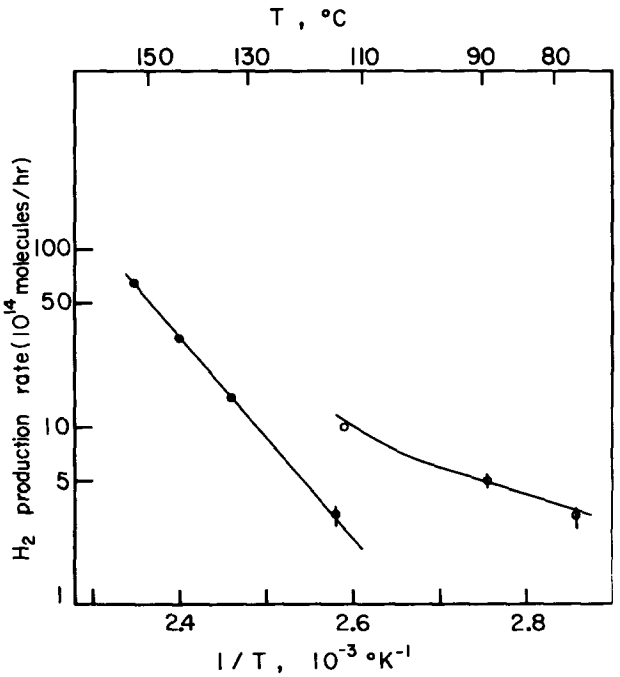

FIG. 4. Arrhenius plot of the rates of photo and thermal water-gas shift reaction over $Pt/TiO_2(100)$ with 18 Torr of water vapor and 0.3 Torr of CO. (○) With uv illumination; (●) without uv illumination.

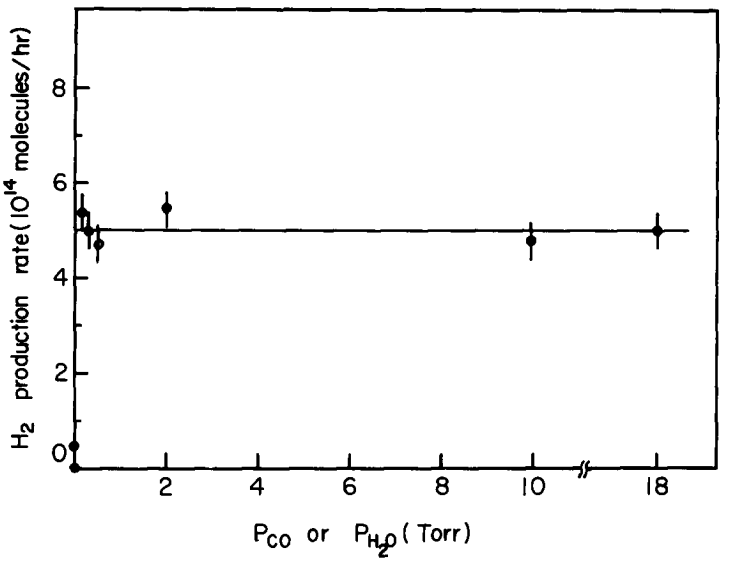

FIG. 5. Hydrogen photoproduction rate over $Pt/TiO_2(100)$ as a function of P_{H_2O} (with P_{CO} = 0.3 Torr; ○) and P_{CO} (with P_{H_2O} = 18 Torr; ●) at 363°K with uv illumination.

rate on uv intensity is shown in Fig. 6. The uv intensity incident on the specimen was varied by placing different wire-mesh filters in front of the focusing optics of the uv mercury lamp, which was kept at a constant input power of 250 W. The wire-mesh filters physically blocked the light evenly over the whole aperture, and their transmissions were measured using a photon power meter. As indicated, the H_2 evolution rate increases monotonically with increasing uv intensity.

3.5. TiO_2 reduction state dependence. The total Pt coverage on the unreduced

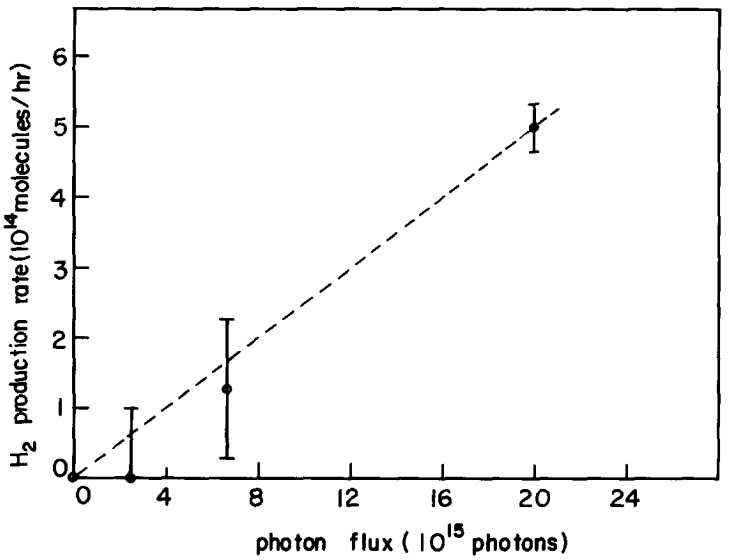

FIG. 6. Hydrogen production rate over $Pt/TiO_2(100)$ at 363°K as a function of uv intensity (P_{H_2O} = 18 Torr, P_{CO} = 0.3 Torr).

$TiO_2(100)$ surface with a surface area of ~ 1.13 cm^2 was 1.8×10^{15} atoms, which corresponds to the standard Pt coverage condition for reduced $TiO_2(100)$. After normalizing the reaction rate to specimen surface area, we found that the reaction proceeded with a transient rate which was only half of that from the reduced surface, while the steady-state reaction rate was the same as that from the reduced surface.

4. DISCUSSION

4.1. *Photocatalytic Reaction*

As mentioned in the introduction, an important point to be established in the photodecomposition of gas-phase water is its photocatalytic nature. A reasonable criterion is that one must produce more than the equivalent of one monolayer of products. Assuming that one monolayer of H_2 corresponds to 10^{15} H_2 molecules/cm^2 surface area of catalyst, one equivalent monolayer would correspond to 6.3×10^{14} H_2 molecules in our experiment with a specimen surface area of 0.63 cm^2. Under optimum conditions, the equivalent of 0.9 monolayer of H_2 was produced in 1 hr at steady state. It is important to point out that this steady-state rate was still maintained when we terminated the experiment after $3\frac{1}{2}$ hr. Therefore, more than three equivalent monolayers of hydrogen were produced. When the H_2 production from the transient reaction is included, the total hydrogen yield exceeds six monolayers after $3\frac{1}{2}$ hr. The photocatalytic nature of the reaction is thus established.

It is interesting to compare our steady-state reaction rate to that obtained by Sato and White (*9*). Extrapolation of their results gives a hydrogen production rate at 363°K of 6×10^{14} H_2 molecules/hr cm^2, assuming that all surface atoms were illuminated by uv. Because of shadowing, it is unlikely to have all surface atoms exposed to the same uv illumination and the effective area is thus reduced. Therefore, this number should represent a lower limit for the hydrogen photoproduction rate. Our observed rate of 9×10^{14} H_2 molecules/hr cm^2 is close to this lower limit. Furthermore, we found that the steady-state reaction rate was the same for both reduced and unreduced TiO_2 surfaces, while their results indicated that H_2-doped TiO_2 powders (reduced) produced H_2 at rates 10 times higher than undoped TiO_2 powders (unreduced). This may be due to several differences between our system and theirs:

(1) Sato and White used anatase TiO_2 powders, which may present more surface irregularities, whereas single-crystal rutile $TiO_2(100)$ was studied in our work.

(2) Pt deposition was applied differently (photoelectrochemical deposition versus vacuum evaporation).

(3) In our study, platinized TiO_2 preparation was conducted in UHV, followed by *in situ* reaction studies without exposure to the atmosphere. In their case, the specimen was exposed to atmosphere after Pt impregnation.

4.2. *Pt Coverage Dependence*

As indicated in Fig. 3, the hydrogen production rate for metal-free $TiO_2(100)$ surface is less than 1×10^{14} H_2 molecules/hr. Platinum alone could not be responsible for hydrogen production since the reaction requires uv illumination at 363°K, and the activity decreases with increasing Pt coverage. Thus a platinized TiO_2 surface is required for the reaction to proceed. This is consistent with Sato and White's work (*9*). Upon Pt deposition, part of the TiO_2 surface is covered by Pt while part of it remains uncovered. At the periphery of the deposited Pt islands, the chemical environment is quite different from the rest of the surface in the sense that Pt and TiO_2 are in close contact and remain accessible to adsorbed gas molecules. It is therefore possible that the periphery of the Pt islands could be the active sites. If this is indeed the case, the hydrogen production rate would be proportional to the total perimeter of all the Pt islands. Since we are unable to

measure the perimeter of Pt islands directly, a computer simulation was applied to calculate perimeter for different Pt coverages. The computer simulation for Pt deposition was done by randomly putting atoms into grids of a 100 × 100 matrix. By definition, deposition of one monolayer corresponds to putting 10^4 atoms into the matrix. The total perimeter of the resultant metal islands was subsequently deduced by determining the sum of the coordination number of all the Pt atoms at the periphery of Pt islands and subtracting this from (full coordination number) × (number of Pt atoms at the periphery of Pt islands). In this way, a perimeter versus Pt coverage curve was obtained. In order to fit this curve to our experimental data, we set the maximum of this curve to that of the experimental data. An excellent match was obtained by assuming that one monolayer of Pt coverage corresponds to 1.5×10^{15} Pt atoms/cm^2. This value happens to be the packing density of Pt in the (111) plane. It is also close to the packing density of 1.47×10^{15} atoms/cm^2 by accommodating two Pt atoms per unreconstructed unit cell of TiO_2(100). Therefore, the assumption that the Pt–TiO_2 periphery sites are involved in the photoreaction is consistent with our experimental results.

It is interesting to point out that these perimeter effects are also implicated from other studies. Theoretical calculations on the Cu/Ni system by Tersoff and Falicov (*11*) showed that Ni (or Pt) sites of highest coordination tend to be most active on the surface, provided they are accessible to adsorbate molecules, such as the concave sites at surface steps or periphery. Sachtler *et al.* (*12*) observed that deposition of monolayer amounts of inert gold on Pt(100) enhances the dehydrogenation rate of cyclohexene, with a coverage dependence similar to Fig. 3.

4.3. Reaction Mechanism

As indicated in Sato and White's work (*10*), strongly reduced TiO_2 powders can give rise to H_2 production upon uv illumination in the presence of water vapor. They believe that such reaction was caused by noncatalytic reaction of H_2O with an oxygen-deficient TiO_2 surface because oxygen was not produced in the reaction. Kawai and Sakata (*8*) found that this reaction proceeded even without uv illumination at room temperature. Similarly, Ferrer and Somorjai (*13*) observed D_2 photoproduction from D_2O vapor on a reduced $SrTiO_3$(111) crystal at 600°K. The reaction appeared to proceed by incorporating oxygen from the water molecule into the crystal lattice, and the hydrogen production was sustained by diffusion of oxygen vacancies from bulk to surface. All these observations imply that (i) an oxygen-deficient TiO_2 surface is chemically active, and (ii) the removal of oxygen from the catalyst surface is an important step for gaseous water photodecomposition. Sustained hydrogen production from water photodecomposition over TiO_2 should occur if oxygen can be continuously removed from the surface.

If the removal of oxygen from the TiO_2 surface is equivalent to reducing TiO_2 into Ti_2O_3, it is thermodynamically very unfavorable as indicated in the following:

$$2TiO_2(s) \rightarrow Ti_2O_3(s) + \tfrac{1}{2}O_2(g), \qquad \Delta G^\circ = 61.6 \text{ kcal}.$$

This may explain the above-mentioned observation that oxygen production was not observed over uv-irradiated TiO_2 in gaseous water alone. However, this unfavorable thermodynamic condition can be minimized by introduction of CO into the system. Volodin *et al.* (*14*) found that anatase TiO_2 could be reduced by uv illumination in the presence of CO. Indeed, this method was adopted by Kawai and Sakata to reduce their TiO_2 specimen (*8*). Quantitative measurement of this photoreduction rate is not available from the literature, but it appears to be a very slow process based on Kawai and Sakata's work (*8*). It is likely that, in the presence of platinum, the TiO_2

reduction rate might be enhanced at the Pt–TiO_2 periphery. Indeed, by electron diffraction analysis of Pt/TiO_2, Baker *et al.* (*15*) found that Pt catalyzes the reduction of TiO_2 in a hydrogen atmosphere at temperatures above 825°K. XPS study of Pt/TiO_2 by Fung (*16*) showed that heating Pt/TiO_2 in H_2 at 600°C gives rise to Ti^{3+} at the surface, while similar treatments on TiO_2 alone do not produce any appreciable amounts of surface Ti^{3+} (*17*), indicating that Pt in contact with TiO_2 makes the latter more easily reducible.

Based on the above observations, we propose the following reaction mechanism for the photoassisted water gas shift reaction on Pt/TiO_2:

$$h\nu \rightarrow h + e, \quad (1)$$

$$Pt/Ti^{4+}\text{–}O^{2-} + 2h + CO_{ads} \xrightarrow{k} Pt/Ti^{4+}\text{–}\square s + CO_2(g), \quad (2)$$

$$Pt/Ti^{4+}\text{–}\square s + H_2O_{ads} + 2e \rightarrow Pt/Ti^{4+}\text{–}O^{2-} + H_2(g). \quad (3)$$

Here $\square s$ signifies an oxygen vacancy on the surface, and $Pt/Ti^{4+}\text{–}O^{2-}$ represents the Pt–TiO_2 periphery site. Based on the above discussion, reaction (3) should be fast. It should be pointed out here that in reaction (2) the charge associated with oxygen ion should not be taken too seriously. Oxygen ion has a -2 charge only when it is fully ionized. Considering the ionic character of TiO_2 (about 63% using Pauling electronegativity), the charge on the oxygen ion should be close to -1. Further, even if two holes are required in reaction (2), they would probably be added in two steps, one of which can be assumed to be rate-determining. In either case, one can show that the rate of hydrogen production r is given by

$$r = k[Pt/Ti^{4+}\text{–}O^{2-}]p[CO_{ads}],$$

where k is the rate constant and p is the hole concentration. Assuming that the concentration of $Pt/Ti^{4+}\text{–}\square s$ is negligible, $[Pt/Ti^{4+}\text{–}O^{2-}]$ is proportional to the total perimeter l. Due to the zero-order CO pressure dependence in our pressure range, the $[CO_{ads}]$ term is probably a constant and can be dropped. We hence get the following expression for r:

$$r = k'lp = k''lI,$$

where I is the uv intensity.

Thus this model explains the linear dependence on total platinum island perimeter as described before. As expected, it also predicts that r varies linearly with uv intensity.

The steady-state reaction probability was $\sim 1 \times 10^{-5}$ hydrogen molecules/photon. This value is very small compared to that of the photoelectrolysis of water, which is typically a few percent but can be as high as 0.5 H_2 molecules/photon (*5*). It should be noted that in both systems only charge carriers delivered to the surface can contribute to the photoreaction. In electrochemical cells, where oxidation and reduction sites are spatially separated, charge carriers produced by photons thousands of angstroms beneath the surface can be separated and driven to their respective electrode surfaces due to semiconductor band-bending and there contribute to the reaction. This greatly enhances the quantum yield in photoelectrolysis of water (*18*). In gas-phase reactions using Pt/TiO_2, however, the harvesting of photogenerated charge carriers deep beneath the surface would not be as effective due to lack of spatial separation of reduction and oxidation sites. An upward band bending at the surface increases the surface hole concentration and at the same time suppresses the surface electron concentration and vice versa. Zero band-bending limits charge carrier collection to within one diffusion length from the surface. This ineffectiveness in transporting photogenerated electrons *and* holes to active sites on the same surface may account for the low photon conversion efficiency. The efficiency can be improved significantly by the use of small-particle catalyst systems, as illustrated in Fig. 7 for the case when the

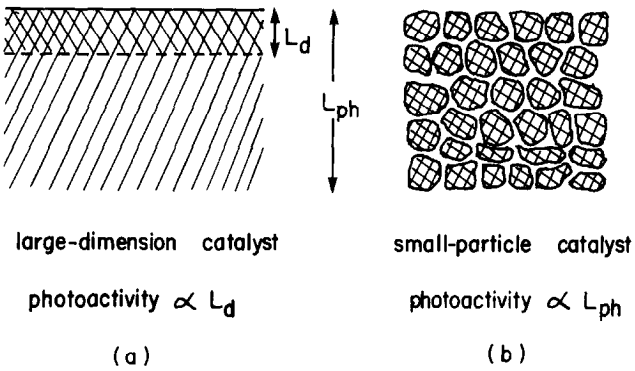

FIG. 7. The comparison of photoactivity for large-dimension catalyst and small-particle catalyst in the case of L_{ph} (photon absorption length) > L_d (charge carrier diffusion length). In (b), the particle size is assumed to be smaller than L_d.

charge carrier diffusion length (L_d) is smaller than the photon absorption length (L_{ph}). For large-particle ($>L_{ph}$) catalysts, charge carriers generated beyond one diffusion length from the surface cannot be utilized. For small-particle ($<L_d$) catalysts, not only is the number of active sites higher, but a much larger fraction of photogenerated charge carriers can diffuse to these sites and contribute to the photoreaction. According to the proposed mechanism, this should result in a proportionally higher photoactivity. Work by Ghosh and Maruska (*19*) showed that the diffusion length for holes in TiO_2 is about 1 μm while the photon absorption length depends on photon energy and can be larger than 1 μm for photon energies less than 3.3 eV. Therefore, to efficiently utilize the uv light, the catalyst particle size should not exceed twice the diffusion length for charge carriers, i.e., about 2 μm. The case when L_d is greater than L_{ph} can be considered similarly. In addition, by working with oxides that are more easily reducible, the rate constant k in reaction (2) may be increased further. Powdered ferric oxide (Fe_2O_3) appears to fit these criteria well and has the additional advantage of a lower band gap (2.2 eV). We are currently pursuing further photo-experiments with this system.

ACKNOWLEDGMENTS

This work was supported by the Division of Basic Energy Sciences, U.S. Department of Energy, under Grant DE-AC02-78ER4946. The measurements were carried out in the Surface Science Facility of Northwestern University's Materials Research Center, supported in part under the NSF-MRL program (Grant DMR79-23573).

REFERENCES

1. Fujishima, A., and Honda, K., *Nature* **238,** 37 (1972).
2. Tomkiewicz, M., and Fay, H., *Appl. Phys.* **18,** 1 (1979).
3. Maruska, H. P., and Ghosh, A. K., *Solar Energy* **20,** 443 (1978).
4. Rajeshwar, K., Singh, P., and Dubow, J., *Electrochim. Acta* **23,** 1117 (1978).
5. Wrighton, M. S., Ellis, A. B., Wolczanski, P. T., Morse, D. L., Abrahamson, H. B., and Ginley, D. S., *J. Amer. Chem. Soc.* **98,** 2774 (1976).
6. Schrauzer, G. N., and Guth, T. D., *J. Amer. Chem. Soc.* **99,** 7189 (1977).
7. Van Damme, H., and Hall, W. K., *J. Amer. Chem. Soc.* **101,** 4373 (1979).
8. Kawai, T., and Sakata, T., *Chem. Phys. Lett.* **72,** 87 (1980).
9. Sato, S., and White, J. M., *J. Amer. Chem. Soc.* **102,** 7206 (1980).
10. Sato, S., and White, J. M., *Chem. Phys. Lett.* **72,** 83 (1980).
11. Tersoff, J., and Falicov, L. M., *Phys. Rev. B* **24,** 754 (1981).
12. Sachtler, J. W. A., Biberian, J. P., and Somorjai, G. A., *Surf. Sci.* **110,** 43 (1981).

13. Ferrer, S., and Somorjai, G. A., *J. Phys. Chem.* **85,** 1464 (1981).
14. Volodin, A. M., Cherkashin, A. E., and Zakharenko, V. S., *React. Kinet. Catal. Lett.* **11,** 235 (1979).
15. Baker, R. T. K., Prestridge, E. B., and Garten, R. L., *J. Catal.* **56,** 390 (1979).
16. Fung, S. C., *J. Catal.* **76,** 225 (1982).
17. Xiong, G., Kao, C. C., Tsai, S. C., and Chung, Y. W., unpublished results.
18. Wagner, F. T., and Somorjai, G. A., *J. Amer. Chem. Soc.* **102,** 5494 (1980).
19. Ghosh, A. K., and Maruska, H. P., *J. Electrochem. Soc.* **124,** 1516 (1977).